Steepest descent reaction path integration using a first-order predictor–corrector method

Hrant P. Hratchian,[1,a] Michael J. Frisch,[1] and H. Bernhard Schlegel[2]
[1]*Gaussian, Inc., 340 Quinnipiac Street, Building 40, Wallingford, Connecticut 06492, USA*
[2]*Department of Chemistry, Wayne State University, Detroit, Michigan 48202, USA*

(Received 8 September 2010; accepted 20 October 2010; published online 8 December 2010)

The theoretical treatment of chemical reactions inevitably includes the integration of reaction pathways. After reactant, transition structure, and product stationary points on the potential energy surface are located, steepest descent reaction path following provides a means for verifying reaction mechanisms. Accurately integrated paths are also needed when evaluating reaction rates using variational transition state theory or reaction path Hamiltonian models. In this work an Euler-based predictor–corrector integrator is presented and tested using one analytic model surface and five chemical reactions. The use of Hessian updating, as a means for reducing the overall computational cost of the reaction path calculation, is also discussed. © *2010 American Institute of Physics*. [doi:10.1063/1.3514202]

I. INTRODUCTION

The reaction path is a central concept in the theoretical description of chemical reactivity, and is given by the curve traced across the Born–Oppenhiemer potential energy surface (PES) as nuclei rearrange and move from one minimum (reactant) to another (product).[1–5] This path, which may include one or more transition structures (TSs) and intermediates, describes the reaction mechanism. With a well-integrated reaction pathway, statistical models can be used to evaluate reaction rates and quantitatively understand how reaction mechanisms proceed.[6–11] The highest energy point along the path connecting reactant to product is the TS, which is a single-geometry representation of the transition state region. Because it lies on the lowest energy path between two minima, it corresponds to a stationary point on the PES with one, and only one, negative second-derivative eigenvalue. The eigenvector associated with this negative eigenvalue is known as the transition vector and is tangent to the reaction path.

Specific definitions of the reaction path vary, but for the purposes of this work it is taken to be the steepest descent pathway initiating from the TS along the transition vector (in both directions). Defining s as the reaction coordinate, or arc length along the path, the steepest descent reaction pathway is defined according to

$$\frac{d\mathbf{x}}{ds} = -\frac{\mathbf{g}(\mathbf{x})}{|\mathbf{g}(\mathbf{x})|}, \tag{1}$$

where $\mathbf{x}$ is the vector of coordinates and $\mathbf{g}$ is the energy gradient at $\mathbf{x}$. When defined in terms of mass-weighted Cartesian coordinates, the steepest descent reaction pathway is also known as the intrinsic reaction coordinate (IRC).[12]

Integration of the IRC requires care as Eq. (1) is a stiff differential equation, and methods for integrating steepest descent paths have been extensively reviewed.[1–5] Both explicit and implicit integrators have been used. An explicit integrator determines the end-point of each step using only information from the current point, while implicit integrators are written in terms of data at both the current and next points. For this reason, implicit integrators are somewhat more difficult to implement and typically include an iterative optimization procedure, though they tend to enjoy greater numerical stability and one is often able to use larger integration step sizes without loss of accuracy relative to a similar explicit method.[13] Some common explicit integrators used to solve IRCs include Euler integration, Ishida–Morokuma–Komornicki (stabilized Euler) method,[14,15] Runge–Kutta (RK)[16,17] and Runge–Kutta–Fehlberg schemes,[18] Page and McIver's local quadratic approximation (LQA),[19,20] and the modified LQA of Sun and Ruedenberg[21,22] and Eckert and Werner.[23] Explicit reaction path following integrators based on classical dynamics have also been reported, and include the dynamic reaction path[24] and damped velocity Verlet methods.[25]

Widely used implicit integrators include the Müller–Brown implicit Euler scheme[26] and the second-order implicit trapezoid method of Gonzalez and Schlegel (GS2).[27,28] Gonzalez and Schlegel also described a family of higher-order implicit integrators.[29] More recently, Burger and Yang reported an interesting algorithm that switches between RK and GS2 integrators depending on the stiffness of Eq. (1).[30] This method takes advantage of the fact that the IRC is not very stiff over much of the path. As a result, implicit integrators, which may require multiple optimization iterations together with multiple energy and derivative evaluations, are often unnecessary for large regions of the reaction path. Therefore, the extra cost of using an implicit integrator is reserved for those integration steps where it is needed. They have also generalized the implicit RK method beyond second order.[31]

Explicit and/or implicit integrators can be combined to form predictor–corrector integrators. A predictor–corrector scheme is made up of three processes: a predictor step (P) moves from the current point to a guess for the next point, the

[a]Author to whom correspondence should be addressed. Electronic mail: hrant@gaussian.com.

function and any necessary derivatives are evaluated (E), and then the current point is refined by a corrector step (C).[13,32] Often, predictor–corrector integrators follow P–E–C–E or P–E–C type procedures. Note that in the context of predictor–corrector language, implicit integration methods typically follow a P–E–(C–E)^m algorithm where the superscript m indicates that C and E steps are repeated m times.

A few years ago, Hratchian and Schlegel developed a Hessian-based predictor–corrector (HPC) IRC integrator.[33,34] The HPC method uses LQA for the predictor component and a modified Bulirsch–Stoer (mBS) integrator[13,32,35–37] for the corrector portion, and follows a P–E–C scheme. The efficiency of the HPC method comes from the use of surface fitting during the C steps. In particular, data from the P step is used to form a distance weighted interpolant (DWI) surface on which the mBS integration is carried out. For studies using *ab initio* model chemistries, this procedure essentially reduces the cost of the corrector integrator to zero. Thus, the stability and accuracy afforded by predictor–corrector integration (relative to integration using a related explicit integrator) are gained absent additional computational cost. As compared to the widely used GS2 method, this savings can be quite meaningful. While both methods can be used with similar integration step sizes,[33,34] GS2 typically requires 3–5 E steps per integrated IRC point; again, HPC only requires a single E step for each IRC point. Another important aspect of the HPC integrator is that the P and the C steps are coupled through the surface fitting procedure. Although mBS is formally an explicit method, in the context of the HPC scheme the mBS is dependent on the predictor end-point as the C integration is done on the fitted surface defined in terms of this P step. In this way, two explicit integrators are coupled to form a predictor–corrector propagation scheme.

In this paper, a P–E–C predictor–corrector method combining the Euler explicit integrator (for the P step) and the mBS scheme (for the C step) is proposed. The E step is used to fit a local DWI surface, on which the C integration is carried out. As with the HPC method, the integrator presented here requires only one evaluation of the energy and derivatives per integrated point on the IRC. This Euler predictor–corrector (EulerPC) integrator is tested on a model PES as well as a set of five chemical reactions. The DWI surfaces used during the C components employ energy second derivatives, and these tests are initially carried out using analytic Hessians evaluated during each E step. The use of Hessian updating with EulerPC reaction path following is also explored.

II. METHODS

The EulerPC integrator presented here is conceptually similar to the HPC integrator[33,34] and other predictor–corrector schemes used in *ab initio* classical trajectory calculations.[38,39] As mentioned above, the EulerPC algorithm is a P–E–C type predictor–corrector method. The P step uses Euler integration, the results of the E step are used to fit a local surface, and the C step refines the P result using mBS integration on the fitted local surface. Memory and central processing unit (CPU)costs for both the predictor and corrector integrators (components 1 and 3) scale as $\mathcal{O}(N_{\text{Atoms}})$, where N_{Atoms} is the number of atoms. In this paper, the surface fitting portion of the algorithm is done using DWIs,[40–43] which requires $\mathcal{O}(N_{\text{Atoms}}^2)$ storage and work. On the other hand, the HPC integrator, which requires diagonalization of the second derivative matrix, has a CPU cost that scales as $\mathcal{O}(N_{\text{Atoms}}^3)$.

The starting point for the EulerPC method is to expand the energy to first-order in the atomic center coordinates, $\mathbf{x}$, substitute this approximate energy into Eq. (1), and integrate with a step size of Δs to yield

$$\tilde{\mathbf{x}}_{i+1} = \mathbf{x}_i - \frac{\mathbf{g}_i}{|\mathbf{g}_i|}\Delta s, \tag{2}$$

where $\tilde{\mathbf{x}}_{i+1}$ will later be corrected by the mBS step.

The Bulirsch–Stoer method is fully described elsewhere.[32,35–37] Briefly, this algorithm integrates over a given interval (set equal to the distance from $\mathbf{x}_i$ to $\tilde{\mathbf{x}}_{i+1}$ in the present case) with some step size h. Then, using a smaller step size reintegrates over the same interval. The results of these two integrations are then fit as a function(s) of h and extrapolated to $h = 0$. If the truncation error of this extrapolation is less than a user-defined threshold the extrapolated result is taken as the final integration solution, $\mathbf{x}_{i+1}$; otherwise, the integration is done again with a smaller step size and the extrapolation carried out with a higher-order polynomial. This process is repeated until the truncation error falls below the threshold. Tests shown later employ a threshold of 1×10^{-6} amu$^{1/2}$ bohr. The size of h is determined by the total integration interval and a defined number of steps, n_h, which increases with each mBS cycle. In the present work, a sequence based on that originally proposed by Bulirsch and Stoer is employed: $\mathbf{n}_h = \{48, 64, 96, 128, \ldots\}$.[32,35–37] The mBS scheme used here differs from the conventional Bulirsch–Stoer method in that simple Euler, rather than modified-midpoint, integration is used. This modification has been made because the stiff nature of Eq. (1) in some regions of the reaction path is significantly magnified with modified-midpoint integration, while Euler integration is much better behaved in the same regions. Readers interested in the complete justification of mBS for reaction path following are referred to previous work.[33]

Over the course of a complete reaction path integration, the mBS integration will require a large number of function evaluations. For this reason, the corrector integration cannot be carried out on the actual PES. Instead, a local surface is fit to the data from the predictor step, across which mBS integration is efficiently applied. Following the HPC scheme, the present method employs DWI surfaces, which have successfully been used in a number of applications.[40–44] The energy on the DWI surface, E_{DWI}, at position $\mathbf{x}$ is written as a linear combination of Taylor series expanded about the N_{data} data points,

$$E_{\text{DWI}} = \sum_{i=1}^{N_{\text{data}}} w_i T_i, \tag{3}$$

where w_i and T_i are the weight and Taylor series values about data point i. Each Taylor series is expanded to second order

$$T_i(\Delta \mathbf{x}_i) = E_i + \mathbf{g}_i^{\mathbf{t}} \Delta \mathbf{x}_i + \tfrac{1}{2} \Delta \mathbf{x}_i^t \mathbf{H}_i \Delta \mathbf{x}_i, \tag{4}$$

where

$$\Delta \mathbf{x}_i = \mathbf{x} - \mathbf{x}_i. \tag{5}$$

In Eqs. (4) and (5), $\mathbf{x}_i$, E_i, $\mathbf{g}_i$, and $\mathbf{H}_i$ are the coordinate vector, energy, gradient, and Hessian at data point i on the PES. In the present work, the weights used in Eq. (3) are given by

$$w_i = \frac{1}{|\Delta \mathbf{x}_i|^2} \left(\sum_{j=1}^{N_{\text{data}}} \frac{1}{|\Delta \mathbf{x}_j|^2} \right)^{-1} \tag{6}$$

which, after some algebraic manipulation, can be reformulated to avoid division by zero. In the case where $N_{\text{data}} = 2$, the two weighting functions are

$$w_1 = \frac{|\Delta \mathbf{x}_2|^2}{|\Delta \mathbf{x}_1|^2 + |\Delta \mathbf{x}_2|^2}, \qquad w_2 = \frac{|\Delta \mathbf{x}_1|^2}{|\Delta \mathbf{x}_1|^2 + |\Delta \mathbf{x}_2|^2}. \tag{7}$$

Note that the first fitting data point is the fully refined point from the previous C step and the second fitting data point is the current P step end-point. Therefore, the gradient used in solving Eq. (1) during mBS integration, and thus the mBS solution itself, depends on $\tilde{\mathbf{x}}_{i+1}$ given by the predictor integrator. Also note that despite use of second derivative information in the DWI fitting procedure, EulerPC is nevertheless a first-order method as the truncation error is dictated by the actual integration and not the form of the fitted surface.

III. NUMERICAL TESTS

Calculations using the EulerPC IRC integrator have been carried out using the development version of the GAUSSIAN program suite.[45] The integrator has been tested using the two-dimensional Müller–Brown surface and five chemical PESs. The chemical reactions considered are HCN → HNC, $H_3CCH_2F \rightarrow H_2CCH_2 + HF$, $Cl^- + CH_3Cl \rightarrow ClCH_3 + Cl^-$, $H_2COH \rightarrow H_3CO$, and $SiH_2 + H_2 \rightarrow SiH_4$. For the chemical reaction cases, the PM6 semi-empirical method has been employed,[46,47] and the IRCs are integrated using mass-weighted Cartesian coordinates. After considering the performance of the EulerPC integration scheme using analytic Hessians at all IRC points, the quality of EulerPC reaction paths using Hessian updating is considered. When used, Hessian updating has been carried out using Bofill's scheme,[48] which has been shown to perform very well for IRC integration.[34]

A. Müller–Brown surface

The Müller–Brown (MB) surface is often used to test reaction path following methods. In terms of two parameters x and y, the MB surface is given by

$$E(x, y) = \sum_i A_i \exp\left[a_i \left(x - x_i^0\right)^2 + b_i \left(x - x_i^0\right)\left(y - y_i^0\right) + c_i \left(y - y_i^0\right)^2 \right] \tag{8}$$

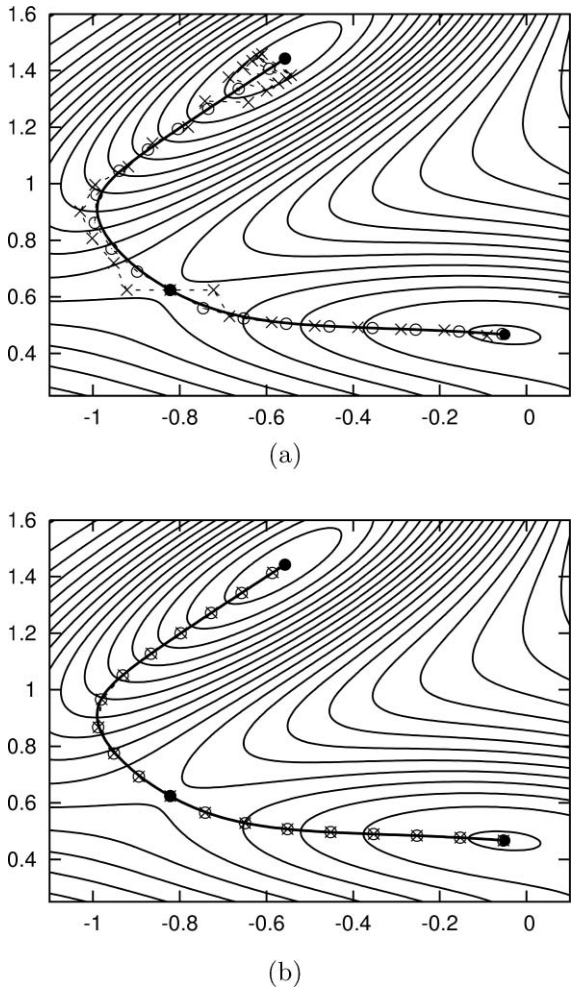

FIG. 1. Reaction path following on the Müller–Brown surface using a step size of 0.10 with (a) Euler (×) and LQA (○) integrators, and (b) EulerPC (×) and HPC (○) integrators. Stationary points are indicated by solid circles and the reference reaction path is given by the solid curve connecting the stationary points. See the text for details.

where

$$\begin{aligned} \mathbf{A} &= \{-200, -100, -170, 15\}, \\ \mathbf{x}^0 &= \{1, 0, -0.5, -1\}, \\ \mathbf{y}^0 &= \{0, 0.5, 1.5, 1\}, \\ \mathbf{a} &= \{-1, -1, -6.5, 0.7\}, \\ \mathbf{b} &= \{0, 0, 11, 0.6\}, \\ \mathbf{c} &= \{-10, -10, -6.5, 0.7\}. \end{aligned} \tag{9}$$

Figures 1 and 2 include contour plots of the MB surface. The region of the surface shown includes the TS at $(-0.822, 0.624)$ and minima at $(-0.558, 1.442)$ and $(-0.050, 0.467)$. These stationary points are indicated in Figs. 1 and 2 by solid circles. A reference reaction path has been integrated using Euler integration with a step size of 0.01, and this reference path is given in the figures by the thick solid curve. The path leading from the TS to the minimum at $(-0.558, 1.442)$ passes through a region of significant curvature. As shown in Figs. 1(a) and 2(a), the first-order

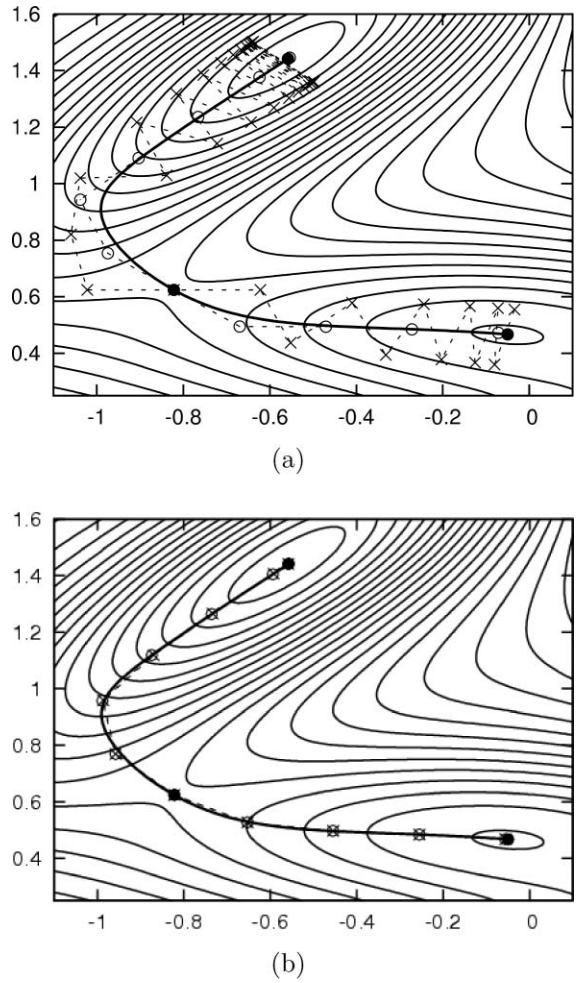

FIG. 2. Reaction path following on the Müller–Brown surface using a step size of 0.20 with (a) Euler (×) and LQA (○) integrators, and (b) EulerPC (×) and HPC (○) integrators. Stationary points are indicated by solid circles and the reference reaction path is given by the solid curve connecting the stationary points. See the text for details.

Euler integrator is unable to follow the reaction path in this region; with a step size of 0.20 (Fig. 2) Euler integration yields a path that suffers from large oscillations about the IRC. The second-order LQA integrator follows the reaction pathway quite closely for the smaller 0.10 step size [Fig. 1(a)]. For the larger 0.20 step size [Fig. 2(a)] LQA experiences minor difficulties following the reaction path through the region of strong curvature, but is able to smoothly right itself back to the reference path in short order. Figures 1(b) and 2(b) display paths using the related predictor–corrector integrators. As shown, EulerPC and HPC results using step sizes of both 0.10 and 0.20 are in excellent agreement with the reference reaction path.

These results on the MB surface clearly indicate the usefulness of predictor–corrector integrators. While the corrector integration component does not change the formal order of the error term, it does significantly reduce the magnitude of the error term prefactor. As a result, the EulerPC first-order integrator yields results that are better than the second-order LQA integrator.

TABLE I. RMS and maximum integration errors for reaction paths solved using EulerPC with analytic Hessians at all predictor integration steps.[a]

Reaction	N_{Steps}	Error RMS	Error Max
Step size = 0.10 amu$^{1/2}$ bohr			
$HCN \rightarrow HNC$	61	0.0002	0.0002
$H_3CCH_2F \rightarrow H_2CCH_2 + HF$	61	0.0002	0.0007
$Cl^- + CH_3Cl \rightarrow ClCH_3 + Cl^-$	26	0.0001	0.0003
$H_2COH \rightarrow H_3CO$	31	0.0001	0.0002
$SiH_2 + H_2 \rightarrow SiH_4$	36	0.0003	0.0009
Step size = 0.40 amu$^{1/2}$ bohr			
$HCN \rightarrow HNC$	15	0.0020	0.0027
$H_3CCH_2F \rightarrow H_2CCH_2 + HF$	15	0.0048	0.0106
$Cl^- + CH_3Cl \rightarrow ClCH_3 + Cl^-$	7	0.0020	0.0037
$H_2COH \rightarrow H_3CO$	8	0.0010	0.0016
$SiH_2 + H_2 \rightarrow SiH_4$	9	0.0059	0.0111

[a]Errors are reported in units of amu$^{1/2}$ bohr. N_{Steps} gives the number of integration steps included in the error analysis.

B. Chemical reaction tests using analytic Hessians

Having demonstrated the accuracy of the EulerPC integrator on the MB surface, we now consider five chemical reactions. In this subsection, energy second derivatives have been evaluated analytically at all predictor integration steps. For each reaction, EulerPC pathways have been integrated using step sizes of 0.10 and 0.40 amu$^{1/2}$ bohr. For comparison, reaction paths using Euler integration with a step size of 0.40 amu$^{1/2}$ bohr are also considered. IRCs integrated using HPC with a step size of 0.02 amu$^{1/2}$ bohr and analytic second derivatives at all predictor integrator points are used as essentially exact solutions to Eq. (1) and are referred to as reference reaction paths in the following discussion.

To quantify the accuracy of the EulerPC integrated reaction pathways, the perpendicular distance from each EulerPC IRC point to the reference reaction path has been computed and root-mean-squared (RMS) and maximum errors are included in Table I. Near the reactant and product basins, these errors can become artificially high due to slightly different ending points. Therefore, this analysis has been carried out specific distances downhill in each direction from the TS: (1) $HCN \rightarrow HNC$ errors are evaluated over $-3.0 \leq s \leq 3.0$ amu$^{1/2}$ bohr; (2) $H_3CCH_2F \rightarrow H_2CCH_2 + HF$ errors are evaluated over $-3.0 \leq s \leq 3.0$ amu$^{1/2}$ bohr; (3) $Cl^- + CH_3Cl \rightarrow ClCH_3 + Cl^-$ errors are evaluated over $0 \leq s \leq 2.5$ amu$^{1/2}$ bohr; (4) $H_2COH \rightarrow H_3CO$ errors are evaluated over $-1.5 \leq s \leq 1.5$ amu$^{1/2}$ bohr; and (5) $SiH_2 + H_2 \rightarrow SiH_4$ errors are evaluated over $-1.5 \leq s \leq 2.0$ amu$^{1/2}$ bohr. In all cases, these limits are located roughly halfway between the inflection and end points in each direction on the reaction path.

Numerically, the order of an integrator can be tested by evaluating the growth of the average error as a function of the integration step size. For an nth-order integrator, the error will increase as the step size raised to the $n+1$ power. The increases in error with step size reported in Table I are consistent with a first-order integrator. Indeed, for each reaction the leading error term is second-order in the step size (increasing the error by roughly a factor of 16 as one increases

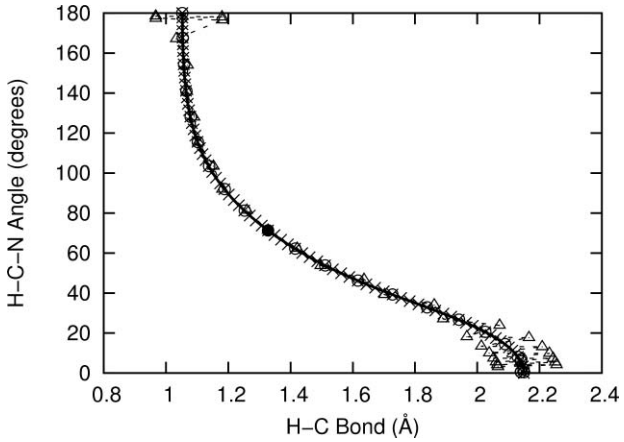

FIG. 3. HCN angle vs C–H bond distance along the HCN → HNC reaction pathway using the EulerPC integration and step sizes of 0.10 (×) and 0.40 (○) amu$^{1/2}$ bohr. Results of Euler integration using a step size of 0.40 amu$^{1/2}$ bohr are also shown (△). The reference reaction path results are given by the solid curve.

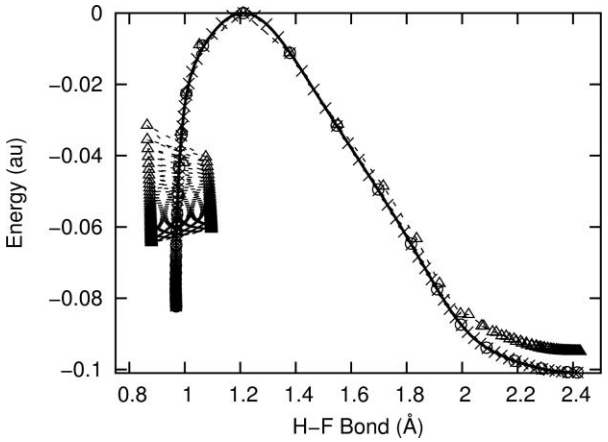

FIG. 4. Four center elimination reaction pathway using the EulerPC integration and step sizes of 0.10 (×) and 0.40 (○) amu$^{1/2}$ bohr. Results of Euler integration using a step size of 0.40 amu$^{1/2}$ bohr are also shown (△). The reference reaction path results are given by the solid curve.

Δs from 0.10 to 0.40 amu$^{1/2}$ bohr). Following the same error analysis procedure, integration errors for these test reactions have also been compiled using step sizes of 0.20 and 0.30 amu$^{1/2}$ bohr. Using the four average RMS errors (over the five test reactions) and plotting ln (error) as a function of ln (Δs) gives a line with slope 2.016, clearly indicating that EulerPC is a first-order integration method.[49]

The first reaction tested was the rearrangement rection of HCN. Figure 3 gives the H–C–N angle as a function of the H–C bond length. It is seen that EulerPC integration using step sizes of 0.10 and 0.40 amu$^{1/2}$ bohr agrees with the reference IRC calculation. Using Euler integration with a step size of 0.40 amu$^{1/2}$ bohr follows the reference IRC well near the TS. However, as the reactant and product basins are approached the Euler path displays oscillations about the reference path. The $\Delta s = 0.1$ amu$^{1/2}$ bohr EulerPC path exhibits nearly zero error relative to the reference reaction path, and the $\Delta s = 0.40$ amu$^{1/2}$ bohr EulerPC calculation has an RMS error of only 0.0020 amu$^{1/2}$ bohr and a maximum error of only 0.0027 amu$^{1/2}$ bohr. These results, for a reaction which involves significant coupling of Cartesian coordinates as the H atom moves from one side of the C–N bond to the other, indicate how accurately the EulerPC method integrates reaction paths.

The four center elimination reaction $CH_3CH_2F \rightarrow CH_2CH_2 + HF$, which has been extensively studied by Kato and Morokuma,[50] has been used in previous studies of reaction path following methods. Figure 4 gives the energy along the reaction path as a function of the H–F bond distance. With an integration step size of 0.40 amu$^{1/2}$ bohr, Fig. 4 shows that simple Euler integration separates from the reference path only slightly as the path is integrated from the TS to the reactant well (CH_3CH_2F). As the Euler integration approaches the product well, the resulting path suffers from excessive H–F bond vibration. On the other hand, the results shown in Fig. 4 indicate that EulerPC integration yields accurate reaction paths using both tested step sizes.

As with the HCN rearrangement reaction, the four center elimination reaction also shows essentially zero error in the $\Delta s = 0.1$ amu$^{1/2}$ bohr case. The larger step size comes with larger RMS and maximum errors of 0.0048 and 0.0106 amu$^{1/2}$ bohr. While these errors appear relatively large, in absolute terms they are quite low, particularly given that a step size of 0.40 amu$^{1/2}$ bohr is much larger than one typically expects to use in practice.

The third test reaction is the symmetric S_N2 reaction of chloride and methylchloride. This reaction path is known to be difficult for IRC integrators,[51] and as such is an excellent test case for new methods. Near the TS, integration of the reaction path can be quite difficult owing to strong coupling of the path tangent and symmetric C–H stretch coordinates. In Fig. 5 the C–H bond distance is plotted as a function of the C–Cl distance. (Note that only one integration direction from the TS is shown as the reaction path is symmetric about the TS.) Euler integration with a step size of 0.40 amu$^{1/2}$ bohr oscillates across the reference path, resulting from the stiff nature of Eq. (1). EulerPC integration is able to properly follow the reaction path even in the region where the stiff nature of the IRC is most severe. The EulerPC calculation on

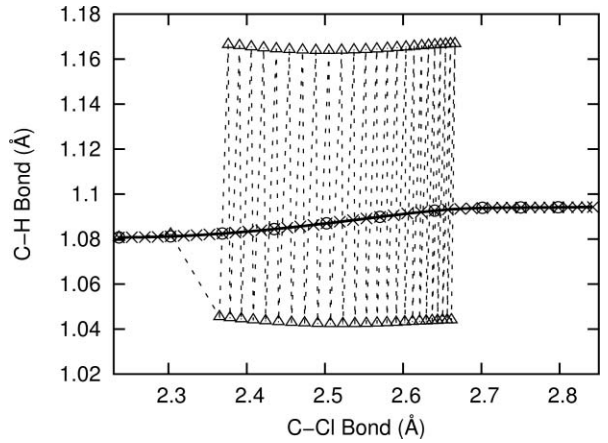

FIG. 5. Reaction path for $Cl^- + H_3CCl \rightarrow ClCH_3 + Cl^-$, using the EulerPC integration and step sizes of 0.10 (×) and 0.40 (○) amu$^{1/2}$ bohr. Results of Euler integration using a step size of 0.40 amu$^{1/2}$ bohr are also shown (△). The reference reaction path results are given by the solid curve.

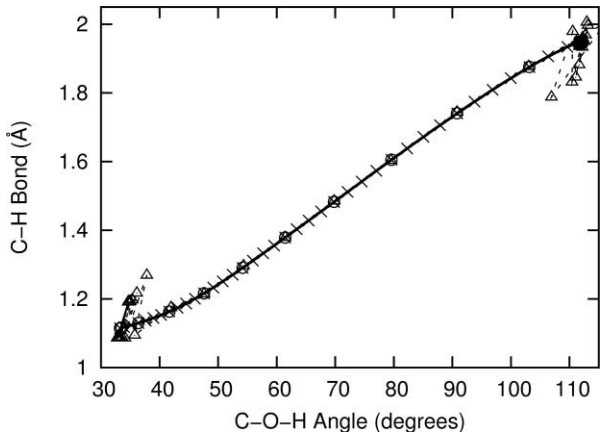

FIG. 6. $H_2COH \rightarrow H_3CO$ reaction path using the EulerPC integration and step sizes of 0.10 (×) and 0.40 (○) $amu^{1/2}$ bohr. Results of Euler integration using a step size of 0.40 $amu^{1/2}$ bohr are also shown (△). The reference reaction path results are given by the solid curve.

this reaction results in RMS and maximum errors of only 0.0020 and 0.0037 $amu^{1/2}$ bohr for the larger integration step size.

The reaction $H_2COH \rightarrow H_3CO$, a 1,2 hydrogen shift reaction, is a model for 1,*n* group shift reactions. Figure 6 shows the C–H distance as a function of the C–O–H angle. Again, the EulerPC integrator results, using step sizes 0.10 and 0.40 $amu^{1/2}$ bohr, clearly follow the reference reaction path. In agreement with this qualitative assessment, the errors of this reaction path (Table I) are quite low. In fact, this test reaction yields the smallest errors of the test set for both $\Delta s = 0.40$ and 0.10 $amu^{1/2}$ bohr cases.

The final chemical reaction considered is $SiH_2 + H_2 \rightarrow SiH_4$, which has been thoroughly studied.[52,53] This reaction serves as a model three center insertion reaction, making it another useful test for new reaction path integrators. Figure 7 is a plot of the H–H bond distance versus the reaction coordinate. Whereas Euler integration incorrectly develops H–H vibrations when entering the reactant channel, the EulerPC solutions cleanly follow the reference IRC.

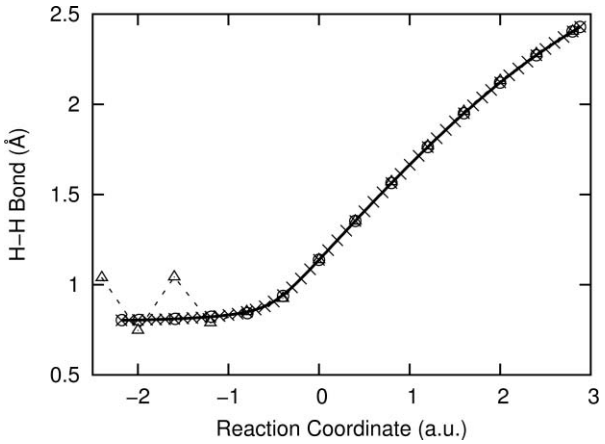

FIG. 7. $SiH_2 + H_2 \rightarrow SiH_4$ reaction path using the EulerPC integration and step sizes of 0.10 (×) and 0.40 (○) $amu^{1/2}$ bohr. Results of Euler integration using a step size of 0.40 $amu^{1/2}$ bohr are also shown (△). The reference reaction path results are given by the solid curve.

The errors of this three center insertion reaction are the largest of the test set. When $\Delta s = 0.10$ $amu^{1/2}$ bohr, the RMS and maximum errors are 0.0003 and 0.0009 $amu^{1/2}$ bohr. With the larger integration step of 0.40 $amu^{1/2}$ bohr the reaction path RMS and maximum errors rise to 0.0059 and 0.0111 $amu^{1/2}$ bohr. As noted above regarding the four center elimination test reaction, errors of this magnitude are not large in an absolute sense. Moreover, the error of the $\Delta s = 0.10$ $amu^{1/2}$ bohr pathway, an accepted step size upper limit in most reaction path following applications, is entirely acceptable.

C. Chemical reaction tests using Hessian updating

As developed thus far, the mBS corrector component of EulerPC integration employs a DWI fitting scheme and requires second derivatives of the energy at each predictor point. Analytic evaluation of second derivatives at each point on the IRC can present a significant computational bottleneck, particularly when *ab initio* (or density functional theory) model chemistries are employed. A commonly used approach for overcoming this bottleneck in quasi-Newton optimization, direct dynamics, and other IRC algorithms is Hessian updating. In this way, the change in the second derivatives with each step is numerically estimated using changes in positions and gradients. Thus, the need for costly analytic second-derivative evaluations at each step is eliminated. In this subsection, such an approach is considered in connection with EulerPC IRC integration.

To quantify the accuracy of the EulerPC integrated reaction pathways when Hessian updating is used, integration errors were determined using a step size of 0.10 $amu^{1/2}$ bohr following the same scheme used for the data given in Table I. Also, the same portions of each reaction path were included in the error analysis: (1) HCN → HNC errors were evaluated for $-3.0 \leq s \leq 3.0$ $amu^{1/2}$ bohr; (2) $H_3CCH_2F \rightarrow H_2CCH_2 + HF$ errors were evaluated for $-3.0 \leq s \leq 3.0$ $amu^{1/2}$ bohr; (3) $Cl^- + CH_3Cl \rightarrow ClCH_3 + Cl^-$ errors were evaluated for $0 \leq s \leq 2.5i$ $amu^{1/2}$ bohr; (4) $H_2COH \rightarrow H_3CO$ errors were evaluated for $-1.5 \leq s \leq 1.5$ $amu^{1/2}$ bohr; and (5) $SiH_4 \rightarrow SiH_2 + H_2$ errors were evaluated for $-1.5 \leq s \leq 2.0$ $amu^{1/2}$ bohr. In each case, this range corresponds to the same number of integration steps as for the all analytic Hessian case (see Table I).

In previous work, it was shown that Hessian updating techniques are quite useful for predictor–corrector reaction path following[34] and direct dynamics methods.[39] Similar to the direct dynamics case, each test chemical reaction has been integrated using an analytic Hessian every two, five, and ten predictor integration steps and updated Hessians at all intermediate steps. Reaction paths have also been integrated using Hessian updating at all integration steps. In all cases, analytic Hessians have been used at the TS, and Hessian updating has been carried out using Bofill's scheme.[48] The root-mean-squared and maximum errors along these integrated reaction paths are given in Table II.

In general, the results shown in Table II are quite good. Using a step size of 0.10 $amu^{1/2}$ bohr the RMS errors are less than 0.002 $amu^{1/2}$ bohr for all cases, including calculations

TABLE II. RMS and maximum integration errors for reaction paths solved using EulerPC with a step size of 0.10 amu$^{1/2}$ bohr incorporating Hessian updating for some or all predictor integration steps.[a]

Reaction	Analytic Hessians every n points			All updated Hessians
	$n = 2$	$n = 5$	$n = 10$	
		RMS error		
$HCN \rightarrow HNC$	0.0002	0.0003	0.0005	0.0013
$H_3CCH_2F \rightarrow H_2CCH_2 + HF$	0.0002	0.0003	0.0008	0.0017
$Cl^- + CH_3Cl \rightarrow ClCH_3 + Cl^-$	0.0001	0.0001	0.0001	0.0003
$H_2COH \rightarrow H_3CO$	0.0001	0.0001	0.0002	0.0003
$SiH_4 \rightarrow SiH_2 + H_2$	0.0003	0.0006	0.0013	0.0014
		Max error		
$HCN \rightarrow HNC$	0.0004	0.0006	0.0010	0.0037
$H_3CCH_2F \rightarrow H_2CCH_2 + HF$	0.0006	0.0006	0.0018	0.0050
$Cl^- + CH_3Cl \rightarrow ClCH_3 + Cl^-$	0.0003	0.0002	0.0004	0.0010
$H_2COH \rightarrow H_3CO$	0.0002	0.0003	0.0004	0.0009
$SiH_4 \rightarrow SiH_2 + H_2$	0.0009	0.0013	0.0028	0.0028

[a]Errors are reported in units of amu$^{1/2}$ bohr.

using all updated Hessians. Similarly, the maximum error values do not exceed 0.005 amu$^{1/2}$ bohr. These error metrics are comparable to those reported for the second-order HPC integrator,[34] which is notable given that EulerPC integration is formally a first-order method. These results further emphasize the usefulness of predictor–corrector integration schemes and the utility of the fitted surface mBS corrector scheme.

IV. CONCLUSIONS

In this work, an Euler-based predictor–corrector (EulerPC) reaction path integrator has been presented. The integrator has been validated on the Müller–Brown surface and with five chemical reactions. In all cases, EulerPC integration yields paths that agree very well with highly accurate reference reaction paths. Integration errors have also been evaluated quantitatively, and it has been shown that the EulerPC integrator performs nearly as well as higher-order schemes. This level of accuracy is achieved because of the corrector integration component. Noting that this integrator has been developed for use in electronic structure studies, this enhancement of accuracy comes without any additional computational cost since the corrector integration is carried out on a fitted surface. It has also been demonstrated that Hessian updating techniques can be successfully employed with EulerPC reaction path following. Hence, the EulerPC integrator is an approach that simultaneously provides a high degree of accuracy and computational affordability.

[1]H. P. Hratchian and H. B. Schlegel, in *Theory and Applications of Computational Chemistry: The First Forty Years*, edited by C. E. Dykstra, G. Frenking, K. S. Kim, and G. E. Scuseria (Elsevier, Amsterdam, 2005) pp. 195–249.
[2]H. B. Schlegel, J. Comput. Chem. **24**, 1514 (2003).
[3]D. J. Wales, *Energy Landscapes* (Cambridge University, Cambridge, 2003).
[4]H. B. Schlegel, in *Encyclopedia of Computational Chemistry*, edited by P. v. R. Schleyer, N. L. Allinger, P. A. Kollman, T. Clark, H. F. Schaefer III, J. Gasteiger, and P. R. Schreiner (Wiley, Chichester, 1998), Vol. **4**, pp. 2432–2437.
[5]M. A. Collins, Adv. Chem. Phys. **93**, 389 (1996).
[6]E. Kraka and D. Cremer, Acc. Chem. Res. **43**, 591 (2010).
[7]E. Kraka, in *Encyclopedia of Computational Chemistry*, edited by P. v. R. Schleyer, N. L. Allinger, P. A. Kollman, T. Clark, H. F. Schaefer III, J. Gasteiger, and P. R. Schreiner (Wiley, Chichester, 1998), Vol. 2, pp. 2437–2463.
[8]B. C. Garrett and D. G. Truhlar, in *Encyclopedia of Computational Chemistry*, edited by P. v. R. Schleyer, N. L. Allinger, P. A. Kollman, T. Clark, H. F. Schaefer III, J. Gasteiger, and P. R. Schreiner (Wiley, Chichester, 1998), Vol. 2, pp. 3094–3104.
[9]D. G. Truhlar, B. C. Garrett, and S. J. Klippenstein, J. Phys. Chem. **100**, 12771 (1996).
[10]D. G. Truhlar and B. C. Garrett, Annu. Rev. Phys. Chem. **35**, 159 (1984).
[11]W. H. Miller, N. C. Handy, and J. E. Adams, J. Chem. Phys. **72**, 99 (1980).
[12]K. Fukui, Acc. Chem. Res. **14**, 363 (1981).
[13]C. W. Gear, *Numerical Initial Value Problems in Ordinary Differential Equations* (Prentice-Hall, Englewood Cliffs, NJ, 1971).
[14]M. W. Schmidt, M. S. Gordon, and M. Dupuis, J. Am. Chem. Soc. **107**, 2585 (1985).
[15]K. Ishida, K. Morokuma, and A. Komornicki, J. Chem. Phys. **66**, 2153 (1977).
[16]K. K. Baldridge, M. S. Gordon, R. Steckler, and D. G. Truhlar, J. Phys. Chem. **93**, 5107 (1989).
[17]B. C. Garrett, M. J. Redmon, R. Steckler, D. G. Truhlar, K. K. Baldridge, D. Bartol, M. W. Schmidt, and M. S. Gordon, J. Phys. Chem. **92**, 1476 (1988).
[18]A. Aguilar-Mogas, X. Gimenez, and J. M. Bofill, Chem. Phys. Lett. **432**, 375 (2006).
[19]M. Page and J. M. McIver, J. Chem. Phys. **88**, 922 (1988).
[20]M. Page, C. Doubleday, and J. W. McIver, J. Chem. Phys. **93**, 5634 (1990).
[21]J. Q. Sun and K. Ruedenberg, J. Chem. Phys. **99**, 5257 (1993).
[22]J. Q. Sun and K. Ruedenberg, J. Chem. Phys. **99**, 5269 (1993).
[23]F. Eckert and H. J. Werner, Theor. Chem. Acc. **100**, 21 (1998).
[24]S. A. Maluendes and M. J. Dupuis, J. Chem. Phys. **93**, 5902 (1990).
[25]H. P. Hratchian and H. B. Schlegel, J. Phys. Chem. A **106**, 165 (2002).
[26]K. Mller and L. D. Brown, Theor. Chim. Acta **53**, 75 (1979).
[27]C. Gonzalez and H. B. Schlegel, J. Chem. Phys. **90**, 2154 (1989).
[28]C. Gonzalez and H. B. Schlegel, J. Phys. Chem. **94**, 5523 (1990).
[29]C. Gonzalez and H. B. Schlegel, J. Chem. Phys. **95**, 5853 (1991).
[30]S. K. Burger and W. T. Yang, J. Chem. Phys. **124**, 224102 (2006).
[31]S. K. Burger and W. T. Yang, J. Chem. Phys. **125**, 244108 (2006).
[32]W. H. Press, *Numerical Recipes in FORTRAN 77: The Art of Scientific Computing*, 2nd ed. (Cambridge University, Cambridge, England; New York, 1996).
[33]H. P. Hratchian and H. B. Schlegel, J. Chem. Phys. **120**, 9918 (2004).
[34]H. P. Hratchian and H. B. Schlegel, J. Chem. Theory Comp. **1**, 61 (2005).
[35]R. Bulirsch and J. Stoer, Numer. Math. **6**, 413 (1964).

[36]R. Bulirsch and J. Stoer, Numer. Math. **8**, 1 (1966).
[37]R. Bulirsch and J. Stoer, Numer. Math. **8**, 93 (1966).
[38]J. M. Millam, V. Bakken, W. Chen, W. L. Hase, and H. B. Schlegel, J. Chem. Phys. **111**, 3800 (1999).
[39]V. Bakken, J. M. Millam, and H. B. Schlegel, J. Chem. Phys. **111**, 8773 (1999).
[40]M. A. Collins, Theor. Chem. Acc. **108**, 313 (2002).
[41]R. P. A. Bettens and M. A. Collins, J. Chem. Phys. **111**, 816 (1999).
[42]K. C. Thompson, M. J. T. Jordan, and M. A. Collins, J. Chem. Phys. **108**, 564 (1998).
[43]J. Ischtwan and M. A. Collins, J. Chem. Phys. **100**, 8080 (1994).
[44]R. Farwig, in *Algorithm for approximation*, edited by J. C. Mason and M. G. Cox (Clarendon, Oxford, 1987) p. 194.
[45]M. J. Frisch, G. W. Trucks, H. B. Schlegel *et al.*, Gaussian Development Version, Revision H.09+, Gaussian, Inc., Wallingford, CT, 2010.
[46]J. J. P. Stewart, J. Mol. Model. **13**, 1173 (2007).
[47]M. Frisch, G. Scalmani, T. Vreven, and G. Zheng, Mol. Phys. **107**, 881 (2009).
[48]J. M. Bofill, J. Comput. Chem. **15**, 1 (1994).
[49]The RMS (maximum absolute) integration errors with a step size of 0.20 $\text{amu}^{1/2}$ bohr are 0.0006 (0.0008), 0.0011 (0.0033), 0.0005 (0.0010), 0.0004 (0.0006), and 0.0014 (0.0037) $\text{amu}^{1/2}$ bohr for HCN → HNC, H_3CCH_2F → H_2CCH_2+ HF, Cl^-+ CH_3Cl → $ClCH_3$+ Cl^-, H_2COH → H_3CO, and SiH_4→ SiH_2+ H_2 test reactions, respectively. The RMS (maximum absolute) integration errors with a step size of 0.30 $\text{amu}^{1/2}$ bohr are 0.0012 (0.0017), 0.0027 (0.0058), 0.0011 (0.0022), 0.0007 (0.0011), and 0.0031 (0.0080) $\text{amu}^{1/2}$ bohr. The average RMS errors used in the ln(error) versus ln(Δs) linear regression are 0.0002 $\text{amu}^{1/2}$ bohr ($\Delta s = 0.10$ $\text{amu}^{1/2}$ bohr), 0.0008 $\text{amu}^{1/2}$ bohr ($\Delta s = 0.20$ $\text{amu}^{1/2}$ bohr), 0.0018 $\text{amu}^{1/2}$ bohr ($\Delta s = 0.30$ $\text{amu}^{1/2}$ bohr), and 0.0033 $\text{amu}^{1/2}$ bohr ($\Delta s = 0.40$ $\text{amu}^{1/2}$ bohr). The linear regression has an R^2 of 0.999.
[50]S. Kato and K. Morokuma, J. Chem. Phys. **73**, 3900 (1980).
[51]A. G. Baboul and H. B. Schlegel, J. Chem. Phys. **107**, 9413 (1997).
[52]P. John and J. H. Purnell, J. Chem. Soc. Faraday Trans. **69**, 1455 (1973).
[53]C. Sosa and H. B. Schlegel, J. Am. Chem. Soc. **106**, 5847 (1984).